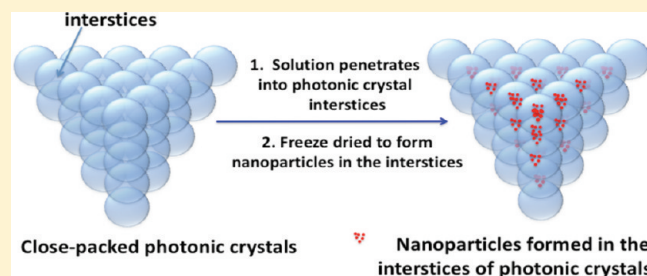


Templated Photonic Crystal Fabrication of Stoichiometrically Complex Nanoparticles for Resonance Raman Solid Cross Section Determinations

Luling Wang, David Tuschel, and Sanford A. Asher*

Department of Chemistry, University of Pittsburgh, Pittsburgh, Pennsylvania 15260, United States

ABSTRACT: Development of methods to fabricate nanoparticles is of great interest for many applications. In this paper, we developed a facile method to fabricate complex stoichiometrically defined nanoparticles by utilizing the defined volume interstices of close-packed photonic crystals. Fabrication of small defined size nanoparticles enables measurements of resonance Raman cross sections of solid materials. We successfully utilized this method to fabricate mixed $\text{NaNO}_3/\text{Na}_2\text{SO}_4$ nanoparticles with a defined stoichiometry on the surface of the photonic crystal spherical particles. We used these stoichiometrically defined $\text{NaNO}_3/\text{Na}_2\text{SO}_4$ nanoparticles to determine the solid UV resonance Raman cross section of the $\text{NO}_3^- \nu_1$ symmetric stretching band (229 nm excitation wavelength) by monitoring the Raman spectrum of Na_2SO_4 as an internal standard. These are the first resonance Raman cross section measurements of solids that avoid the biasing of self-absorption. These $\text{NaNO}_3/\text{Na}_2\text{SO}_4$ nanoparticles appear to show a more facile photolysis than is observed for normal solid NaNO_3 samples. This templated photonic crystal fabrication of complex nanoparticle method will be important for many applications.



INTRODUCTION

There is great interest in fabricating designer nanoparticles (NPs) for numerous applications, including sophisticated photonic crystals (PCs),^{1–6} drug delivery,⁷ bioimaging,⁸ catalysis,⁹ electronics,¹⁰ etc. The fabrication methodologies often require careful control of reaction conditions such as pH,¹ temperature,² reactants,^{1,2} solvents,³ and electric fields.¹¹ In general, it is still difficult to make NPs of most pure materials, and it is especially difficult to make NPs which homogeneously combine materials with defined stoichiometries.

We report here a facile method to fabricate complex stoichiometrically defined NPs by utilizing the defined volume interstices of close-packed PCs as templates within which we form NPs. We fill the PC interstices with a solution containing the materials of interest. We then freeze the solution and then sublime the solvent which leaves the solute NPs within the PC interstices.

The NPs made here are a homogeneous nanomixture of NaNO_3 , an energetic material that we wish to determine the resonance Raman cross section of, and Na_2SO_4 , an internal standard that is transparent and whose solid Raman cross section we recently measured to be $2.74 \times 10^{-28} \text{ cm}^2 \cdot \text{molecule}^{-1} \cdot \text{sr}^{-1}$ at 229 nm excitation.¹² While these solid materials can be mixed, any resonance Raman measurement of the mixtures will be biased because the NaNO_3 particles strongly absorb light and the contribution of NaNO_3 Raman scattering is decreased compared to that of Na_2SO_4 .¹³ What is needed is a nanomixture of the materials in which the NaNO_3 NPs do not significantly attenuate the excitation source traversing the particles. We here demonstrate

a method to form a stoichiometrically defined nanomixture of materials with a particle size from $1 \mu\text{m}$ down to $\sim 1 \text{ nm}$.

For many applications it is possible to utilize or study the NPs within the PC interstices. In the case here, the PC is composed of silica spheres that do not absorb light in the UV, visible, or in most of the IR spectral region.

If necessary, the NPs can be isolated by dissolving the silica spheres in HF. Alternatively, the PC can be prepared from monodisperse polymer spheres that can be dissolved in organic solvent.

EXPERIMENTAL SECTION

Preparation of Close-Packed Silica PCs. Silica NPs were purchased from Allied High Tech Products, Inc. (item # 18050015). The silica NP dispersion was cleaned by six repetitions of the following procedure: the dispersion was centrifuged at 6000 rpm for 20 min, and the pellet was discarded. This dispersion was then centrifuged at 10000 rpm for 30 min. This pellet was collected and redispersed in water. Further purification was achieved by shaking the silica dispersion with mixed bed ion-exchange resin (Bio-Rad AG 501-X8) to remove ionic impurities.

The original silica colloid had a dynamic light scattering (DLS) diameter of 84 nm with a DLS calculated polydispersity of 19.1%. After fractionation the silica colloid had a DLS diameter of 88 nm and a polydispersity of 4.3%. Figure 1a shows the transmission

Received: March 4, 2011

Revised: June 1, 2011

Published: June 06, 2011

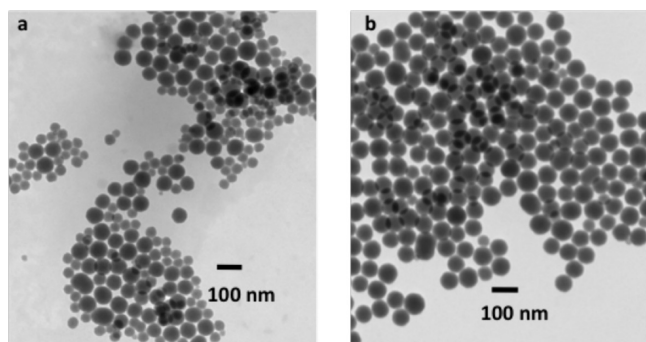


Figure 1. (a) TEM image of original silica colloid. (b) TEM image of silica colloid after cleaning and fractionation.

electron microscopy (TEM) of the original silica colloid while Figure 1b shows a TEM image of fractionated silica colloid which shows a TEM diameter of 73 ± 7 nm. The improved monodispersity is evident, especially the removal of the smaller diameter particles. After being cleaned, these silica particles self-assemble into a crystalline colloidal array (CCA).^{3,14,15}

The close-packed silica PCs were prepared by concentrating the silica CCA solution to 15 wt % silica particles. A 5.75 g portion of this silica CCA in a 10 mL clean beaker was dried at 60 °C in an oven for 24 h. As the solvent evaporated, the silica CCA formed a close-packed PC.¹

Formation of $\text{NaNO}_3/\text{Na}_2\text{SO}_4$ NP in Close-Packed PC Interstices. Fifty milligrams of the silica PCs was placed in a small plastic tube and 8.9 μL of a solution containing NaNO_3 (0.0235 M) and Na_2SO_4 (0.94 M, mole ratio 1:40) was dropped onto the PCs. The solution was sucked into the PC interstices by capillary forces. The PC was then frozen by liquid N_2 and pumped under vacuum for 6 h to sublime the water. During sublimation, $\text{NaNO}_3/\text{Na}_2\text{SO}_4$ composite NPs formed in the interstices. The PC containing $\text{NaNO}_3/\text{Na}_2\text{SO}_4$ NPs was characterized by scanning electron microscopy (SEM) and Raman spectroscopy.

Characterization. DLS was measured by using a Brookhaven Corp. ZetaPALS. For TEM measurements, a few drops of a dilute dispersion of silica NPs were dried on a carbon-coated copper grid (Ted Pella, Inc.) and observed by using a Philips Mogagni 268 TEM. Samples for SEM were sputter-coated with palladium. SEM studies were performed on a Phillips FEG XL-30 FESEM. Optical images of the silica PC were recorded by using a digital stereo zoom microscope (Motic DM-143 series, Ted Pella, Inc.).

Raman of $\text{NaNO}_3/\text{Na}_2\text{SO}_4$ NP in PC Interstices. Raman spectra were excited with the 229 nm line (0.80 mW) of a CW UV Ar laser (Innova 300 FReD, Coherent Inc.).^{16,17} Laser excitation excited the spinning sample approximately in a back-scattering geometry with the laser beam focused to a ~ 20 μm diameter spot. The spinning cell was mounted with its axis of rotation parallel to the optical axis of the collection lens and the cell was spun at >600 rpm. The samples were mounted on the outer ring (1.5 cm diameter, ~ 2 mm wide) of the spinning cell by using double stick tape (3M, Inc.). The Raman light was dispersed by a modified Spex triplemate spectrograph and a Princeton Instruments CCD camera (Spec-10 System, model 735-0001).^{16,17}

RESULTS AND DISCUSSION

We fabricated these mixed $\text{NaNO}_3/\text{Na}_2\text{SO}_4$ composite NP within the defined volume interstices of the close-packed silica PC (Figures 2, 3). The interstices of the PC were filled with a

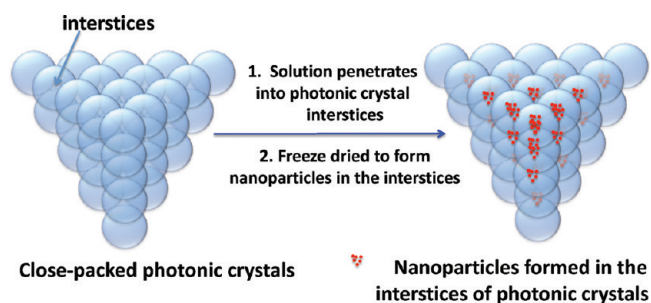


Figure 2. Templated fabrication of nanoparticles in PC interstices.

$\text{NaNO}_3/\text{Na}_2\text{SO}_4$ solution that contained the $\text{NaNO}_3/\text{Na}_2\text{SO}_4$ concentration necessary to form NP of a size equal to the maximum particle size desired. Strong capillary forces sucked the solution into the interstices of the PC. Penetration of the solution was evident since the PC became more transparent as the air was replaced by a solution that better refractive index matched the silica particles. The PC containing the solution was quickly frozen by contact with liquid N_2 . The solvent was sublimated by exposure of the sample to vacuum, leaving behind the NP.

Figure 3a shows a SEM of the close-packed silica PC, while Figure 3b shows an optical micrograph of the PC prior to solution incorporation. The PC is relatively transparent because the particles are small and the PC diffracts light only in the UV.

The PC interstices function as nanodomains that enclose the penetrating solution. The interstitial volume of the close packed PC is 26%.¹⁸ The single interstitial volume (V_{in}) can easily be calculated as: $V_{\text{in}} = (2^{1/2}/6 - \pi/18)D^3$, where D is the close packed sphere diameter. The volume of the solution necessary to completely fill all interstices of the PC, V_{sol} can be calculated from w , the weight of the PC, given that the silica density, ρ , is 2.0 g/mL:¹⁹ $V_{\text{sol}} = 0.35w/\rho$.

We can calculate the maximum diameter of the formed NPs in the interstices from the concentration of nonvaporous species in the solution that fills the interstitial volume. The calculated particle diameter is a maximum since the solids either can agglomerate into one single particle or can form numerous particles or can form arrays of NPs that coat the silica particle surfaces.

The Figure 3c SEM shows that the $\text{NaNO}_3/\text{Na}_2\text{SO}_4$ NP coat the surface of silica particles. Visually we estimate a diameter of ~ 4 nm.

We measured the resonance Raman spectra of the NO_3^- in the PC by exciting at 229 nm within the $\text{NO}_3^- \pi \rightarrow \pi^*$ electronic transition.^{17,20,21} The Figure 3d UV resonance Raman (RR) spectrum shows a dominating 1062 cm^{-1} $\text{NO}_3^- \nu_1$ symmetric stretching vibration²² as well as the 995 cm^{-1} SO_4^{2-} symmetric stretch. The other Raman bands observed are mainly from the double stick tape and from Raman scattering of the silica PC (Figure 3d). The shoulder at $\sim 1653 \text{ cm}^{-1}$ in the PC reference Raman spectrum derives from the degradation of the tape. The spectra in Figure 3d were normalized to the tape 1604 cm^{-1} Raman band.

Because of the small particle sizes, we can ignore the self-absorption by the $\text{NaNO}_3/\text{Na}_2\text{SO}_4$ NPs since we estimate that it would take a ~ 70 nm thick pure NaNO_3 film to absorb 50% of the incident 229 nm excitation light.²¹ We can calculate the solid Raman cross section of the ν_1 symmetric stretch of NO_3^- ($\sigma_{\text{NO}_3^-}$) from the ratio of intensities of the $\text{NO}_3^- \nu_1$ symmetric stretch band ($I_{\text{NO}_3^-}$) to the SO_4^{2-} symmetric stretch

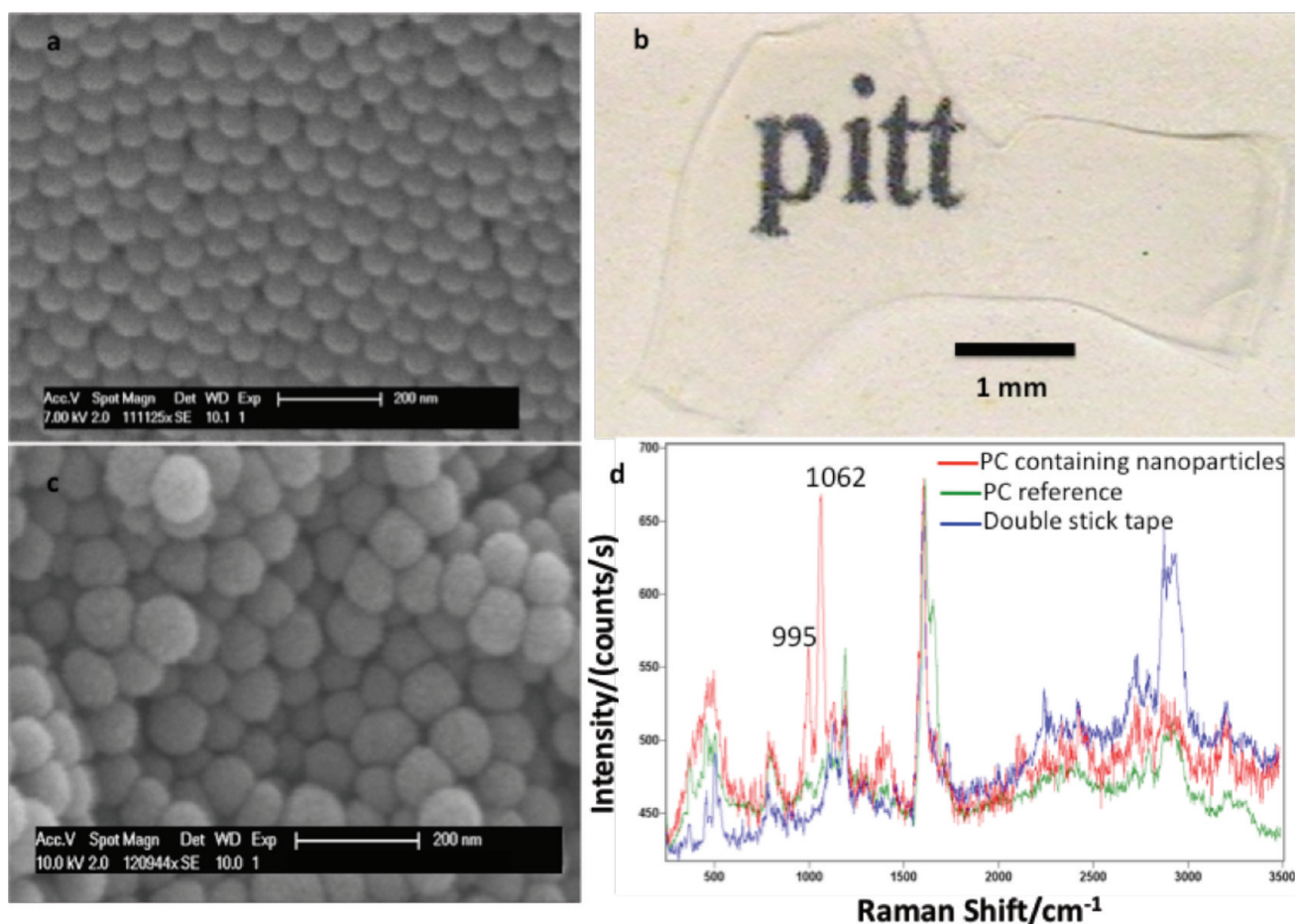


Figure 3. (a) SEM of close-packed PCs. (b) Optical image of the close-packed silica PCs. (c) SEM image of close-packed PCs with NPs (NaNO_3 to Na_2SO_4 mole ratio 1:40) formed in the interstices. (d) Raman spectra of the PCs with NPs in the interstices (red), PC reference (green), and double stick tape.

band ($I_{\text{SO}_4^{2-}}$) by using eq 1.

$$\frac{I_{\text{NO}_3^-}}{I_{\text{SO}_4^{2-}}} = \frac{\sigma_{\text{NO}_3^-} C_{\text{NO}_3^-}}{\sigma_{\text{SO}_4^{2-}} C_{\text{SO}_4^{2-}}} \Rightarrow \sigma_{\text{NO}_3^-} = \frac{I_{\text{NO}_3^-} C_{\text{SO}_4^{2-}}}{I_{\text{SO}_4^{2-}} C_{\text{NO}_3^-}} \sigma_{\text{SO}_4^{2-}} \quad (1)$$

The concentration ratio ($C_{\text{NO}_3^-}/C_{\text{SO}_4^{2-}}$) of the NP is that of the solution that penetrated the PC interstices (1:40). The measured relative intensity ($I_{\text{NO}_3^-}/I_{\text{SO}_4^{2-}}$) of 2.6 was obtained by integrating the Raman bands in Figure 3d. We recently measured a solid state Raman cross section of the 995 cm^{-1} SO_4^{2-} band of $1.96 \times 10^{-28} \text{ cm}^2 \cdot \text{molecule}^{-1} \cdot \text{sr}^{-1}$ with 244 nm excitation.¹² By using the Raman cross section wavelength dispersion,²⁰ we calculated a solid state 229 nm Raman cross section of the 995 cm^{-1} SO_4^{2-} band of $2.74 \times 10^{-28} \text{ cm}^2 \cdot \text{molecule}^{-1} \cdot \text{sr}^{-1}$. From this, we calculate a solid 229 nm resonance Raman cross section for the NO_3^- ν_1 symmetric stretch band of $2.85 \times 10^{-26} \text{ cm}^2 \cdot \text{molecule}^{-1} \cdot \text{sr}^{-1}$.

Thus, we find that the solid state Raman cross section of the NO_3^- ν_1 symmetric stretch band is around 40% of the solution 229 nm Raman cross section of $7.4 \times 10^{-26} \text{ cm}^2 \cdot \text{molecule}^{-1} \cdot \text{sr}^{-1}$.¹⁷ We believe that this is the first solid state resonance Raman cross section measurement for any compound. The fact that the solid state and solution resonance Raman cross sections are different indicates the resonance Raman enhancement is somewhat impacted by interactions

between adjacent electronic transitions of the NO_3^- groups in the lattice, relative to that of the isolated NO_3^- in water.

The solid and solution NO_3^- Raman cross sections are expected to differ because of both chemical and electromagnetic differences. The chemical difference will cause changes in the ground and excited states and shift the transition energies and cause changes in the homogeneous and inhomogeneous line-widths. These effects will also change the relative Raman cross sections between the solution and solid states.

The electromagnetic differences result from the change in the exciting and Raman scattered electric fields in the solution state with refractive index n_s versus the solid state with refractive index of n_c .²³ From the local field corrections we expected to see larger solid nitrate Raman cross section than the solution value because of higher refractive index of the solid materials. However, this is opposite to our experimental results where the solid nitrate Raman cross section is around 40% of the solution value, which indicates that the cross section differences between the pure solid versus the solution are dominated by chemical differences.

This result is important in any understanding of the difference in quantum yields of the photochemical reaction $\text{NO}_3^- + h\nu \rightarrow \text{NO}_2$ that we measured to be 0.04 for NO_3^- dissolved in water but is much smaller with a quantum yield of 10^{-8} for solid NaNO_3 .²⁴ This suggests that the decreased solid state quantum yield may be related to constraints by the NO_3^- surrounding lattice.

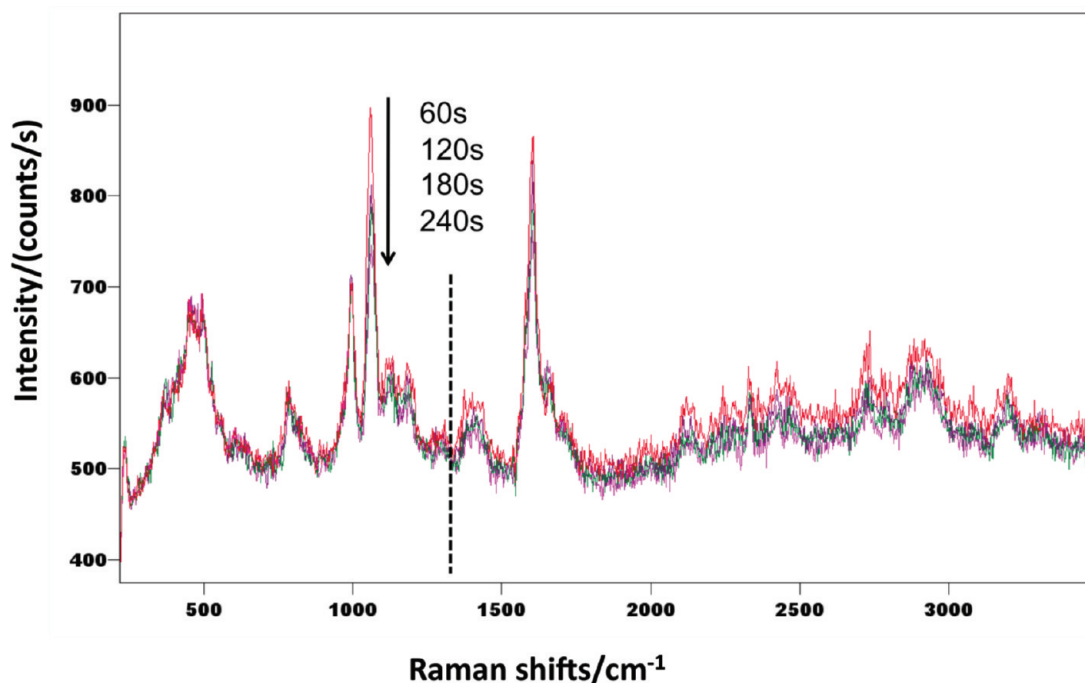


Figure 4. Raman spectra of the $\text{NaNO}_3/\text{Na}_2\text{SO}_4$ nanoparticles (NaNO_3 to Na_2SO_4 mole ratio 1:40) in the PC interstices at illuminating times of 60, 120, 180, and 240 s.

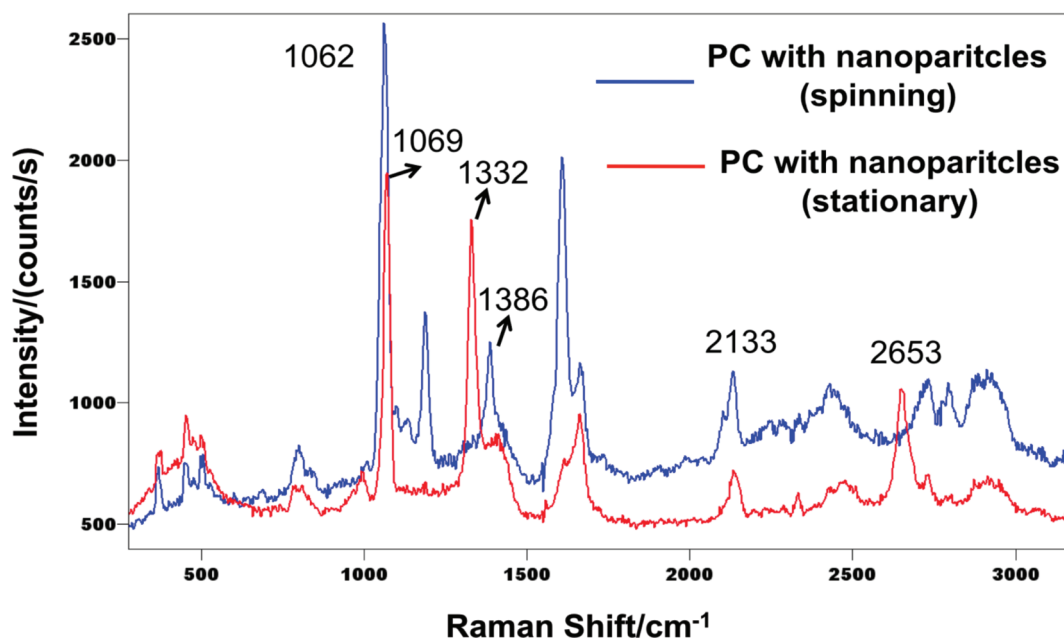


Figure 5. Raman spectra of the $\text{NaNO}_3/\text{Na}_2\text{SO}_4$ nanoparticles (NaNO_3 to Na_2SO_4 mole ratio 1.67:1) in the PC interstices under the spinning (blue) and stationary (red) conditions.

In this regard we see a significantly larger photochemical quantum yield for the $\text{NaNO}_3/\text{Na}_2\text{SO}_4$ NPs than for solid NaNO_3 . Figure 4 shows the illumination time dependence of the 229 nm excited UV resonance Raman spectrum of a spinning sample of the $\text{NaNO}_3/\text{Na}_2\text{SO}_4$ NPs. We observed a significant decrease in the relative intensity of the 1062 cm^{-1} NO_3^- ν_1 symmetric stretching vibration compared to the 995 cm^{-1} SO_4^{2-} symmetric stretch after 60 s of illumination. A spinning

solid NaNO_3 sample shows negligible photochemistry under these conditions.²⁴ It is surprisingly that Figure 4 does not show the ν_1 symmetric stretching band at $\sim 1332\text{ cm}^{-1}$ of NO_2 , the expected photochemical product.

In contrast, the Figure 5 UV resonance Raman spectrum of a stationary sample of the $\text{NaNO}_3/\text{Na}_2\text{SO}_4$ NP clearly shows the NO_2 ν_1 symmetric stretching band at $\sim 1332\text{ cm}^{-1}$ of the photochemical formation of NO_2 . We will investigate the lack

of the $\sim 1332\text{ cm}^{-1}$ NO_2^- band in the spinning samples in future studies. We will also better characterize the photochemical quantum yields of the $\text{NaNO}_3/\text{Na}_2\text{SO}_4$ NPs.

CONCLUSIONS

We developed a facile method of fabricating complex stoichiometry NPs by utilizing the defined volume interstices of close-packed PCs as templates. We successfully utilized this method to fabricate mixed $\text{NaNO}_3/\text{Na}_2\text{SO}_4$ NPs. SEM and Raman spectroscopy show that the $\sim 4\text{ nm}$ mixed $\text{NaNO}_3/\text{Na}_2\text{SO}_4$ NPs formed on the surfaces of the PC spherical particles. By using Na_2SO_4 as an internal standard, we determined that the solid Raman cross section of the NO_3^- ν_1 symmetric band is $2.85 \times 10^{-26}\text{ cm}^2 \cdot \text{molecule}^{-1} \cdot \text{sr}^{-1}$. We also observe much more facile photolysis of the $\text{NaNO}_3/\text{Na}_2\text{SO}_4$ NPs than for solid NaNO_3 . This templated PC fabrication of complex NPs method will be important for many applications, one of which is for determining the resonance Raman cross section of solid materials.

AUTHOR INFORMATION

Corresponding Author

*E-mail: asher@pitt.edu.

ACKNOWLEDGMENT

We acknowledge partial funding of this work by the West Virginia High Technology Consortium Foundation under Contract Number HSHQDC-09-C-00159 from the Department of Homeland Security Science and Technology Directorate. We thank Materials Microcharacterization Laboratory (University of Pittsburgh) for the use of the SEM instrument.

REFERENCES

- (1) Wang, L.; Asher, S. A. *Chem. Mater.* **2009**, *21*, 4608–4613.
- (2) Reese, C. E.; Guerrero, C. D.; Weissman, J. M.; Lee, K.; Asher, S. A. *J. Colloid Interface Sci.* **2000**, *232*, 76–80.
- (3) Wang, W.; Asher, S. A. *J. Am. Chem. Soc.* **2001**, *123*, 12528–12535.
- (4) Xu, X.; Majetick, S.; Asher, S. A. *J. Am. Chem. Soc.* **2002**, *124*, 13864–13868.
- (5) Luo, J.; Qu, D.; Tikhonov, A.; Bohn, J.; Asher, S. A. *J. Colloid Interface Sci.* **2010**, *345*, 131–137.
- (6) Pan, G.; Tse, A. S.; Kesavamoorthy, R.; Asher, S. A. *J. Am. Chem. Soc.* **1998**, *120*, 6518–6524.
- (7) Moinard-Checot, D.; Chevalier, Y.; Briancon, S.; Fessi, H.; Guinebretiere, S. *J. Nanosci. Nanotechnol.* **2006**, *6*, 2664–2681.
- (8) Selvan, S. T.; Tan, T. T. Y.; Yi, D. K.; Jana, N. R. *Langmuir* **2010**, *26*, 11631–11641.
- (9) Toshima, N. *Inorganic Nanoparticles*; CRC Press: Boca Raton, FL, 2011; Chapter 17, pp 475–509.
- (10) Joo, S.; Baldwin, D. F. *IEEE Electron. Compon. Technol. Conf.* **2007**, *1*, 219–226.
- (11) Zhao, H.; Liu, X.; Tse, S. D. *J. Nanopart. Res.* **2008**, *10*, 907–923.
- (12) Wang, L.; Asher, S. A. A Refractive-index Matching Method for Solid UV Raman Cross Section Determinations. *Appl. Spectrosc.*, in preparation.
- (13) Shriver, D. F.; Dunn, J. B. R. *Appl. Spectrosc.* **1974**, *28*, 319–323.
- (14) Carlson, R. J.; Asher, S. A. *Appl. Spectrosc.* **1984**, *38*, 297–304.
- (15) Rundquist, P. A.; Photinos, P.; Jagannathan, S.; Asher, S. A. *J. Chem. Phys.* **1989**, *91*, 4932–4941.
- (16) Asher, S. A.; Bormett, R. W.; Chen, X. G.; Lemmon, D. H.; Cho, N.; Peterson, P.; Arrigoni, M.; Spinelli, L.; Cannon, J. *Appl. Spectrosc.* **1993**, *47*, 628–633.

(17) Tuschel, D. D.; Mikhonin, A. V.; Lemoff, B. E.; Asher, S. A. *Appl. Spectrosc.* **2010**, *64*, 425–432.

(18) Chung, Y. *Introduction to materials science and engineering*; CRC Press: Boca Raton, FL, 2007; p 16.

(19) Jiang, P.; Bertone, J. F.; Hwang, K. S.; Colvin, V. L. *Chem. Mater.* **1999**, *11*, 2132–2140.

(20) Dudik, J. M.; Johnson, C. R.; Asher, S. A. *J. Chem. Phys.* **1985**, *82*, 1732–1740.

(21) Ianoul, A.; Coleman, T.; Asher, S. A. *Anal. Chem.* **2002**, *74*, 1458–1461.

(22) Hickey, L.; Klopogge, J. T.; Frost, R. L. *J. Mater. Sci.* **2000**, *35*, 4347–4355.

(23) Mirone, P. *Spectrochimica Acta* **1966**, *22*, 1897–1905.

(24) Asher, S. A.; Tuschel, D. D.; Vargson, T. A.; Wang, L.; Geib, S. *J. Phys. Chem. A* **2011**, *115*, 4279–4287.